

Length dependent dynamics of microtubules

Vandana Yadav and Sutapa Mukherji

Department of Physics, Indian Institute of Technology, Kanpur-208 016

(Dated: November 10, 2018)

Certain regulatory proteins influence the polymerization dynamics of microtubules by inducing catastrophe with a rate that depends on the microtubule length. Using a discrete formulation, here we show that, for catastrophe rate proportional to the microtubule length, the steady-state probability distributions of length decay much faster with length than an exponential decay as seen in the absence of these proteins.

I. INTRODUCTION

Microtubules are important components of the cytoskeleton of the cell [1]. These are hollow microscopic tubes formed by α , β -tubulin heterodimers. These dimers are joined end-to-end to form protofilaments with alternating α , β subunits. The wall of the microtubule has a staggered arrangement of typically 13 such protofilaments. Experimental observations of the polymerization dynamics of microtubules reveal that microtubules alternate between persistent polymerizing and depolymerizing phases. This unusual feature is known as the "dynamic instability" [2]. The transition from a polymerizing to a depolymerizing phase is known as "catastrophe" and the same from a depolymerizing phase to a polymerizing phase is known as "rescue". A popular idea regarding the cause of the dynamic instability is that it occurs as a result of two competing processes, the addition of GTP bound tubulins at the growing tip and the hydrolysis of the GTP units of the tubulins present on the microtubule [2–4]. The GTP bound tubulins provide a stabilizing cap to the growing end and if this cap is lost due to rapid hydrolysis of the GTP units, the microtubule enters into a depolymerizing phase.

Microtubules are responsible for various intracellular organisation, exerting pushing or pulling forces etc. It is, therefore, important that the polymerization and depolymerization of microtubules are appropriately regulated so that the length distribution of microtubules satisfies the requirement of the cell. It is found that the microtubule dynamics is linked to a large number of regulatory mechanisms of microtubule associated proteins [1]. *In vivo* experiments show that a variety of proteins known as polymerases or depolymerases stabilize or destabilize the microtubules by reducing or enhancing the catastrophe rate [5] respectively. Although the mechanism as exactly how the microtubule associated proteins influence the dynamics is not known, there are experimental evidences of length dependent regulation of microtubule dynamics under different cellular contexts [6–9]. While in certain cases, there are speculations about the microscopic origin of such regulations [6], recent *in vivo* studies on two different systems find depolymerases belonging to kinesin-5 [8] and kinesin-8 [9] family of proteins responsible for such length-dependent regulation. In particular, live-cell imaging of interphase fission yeast cells [9] suggests that

kinesin-8 regulation leads to an increase of the catastrophe frequency with the microtubule length. Since, in this case, the depolymerization is length dependent, cells may selectively control the (de)polymerization dynamics of different populations of microtubules. As a consequence, the activity of such depolymerases is important for formation of ordered microtubule-based structures during cell division. Recent numerical simulations suggest that such length dependent regulation of polymerization dynamics is crucial also for microtubule related processes during cell division [10].

A possible mechanism through which kinesin-8 might introduce a length dependence in the catastrophe frequency has recently been proposed in [11]. The authors of [11] simulate the regulatory mechanism based on the following postulates. The processive depolymerases, after binding, walk towards the plus end of the microtubule and accumulate near its tip. Since these molecules can bind anywhere along the length with equal probability, and unbind rarely, it is likely that longer microtubules have larger density of the proteins at the tip than the shorter ones. Once the motor reaches the tip, it encounters a 'push' from the subsequent motors. A 'pushed' motor at the tip finally breaks off taking the terminal tubulin along with. This gives rise to catastrophe due to the shortening of the GTP cap. These studies indicate that the catastrophe frequency increases linearly with the length of the the microtubule, as observed experimentally from live-cell imaging of fission yeast cells [9].

In the context of such dynamic instability, the central properties of interest are the length distributions of a set of microtubules [12, 13]. Apart from being useful for obtaining various statistical averages as a function of the rate parameters, these distributions lead to predictions of various quantities such as microtubule's mean life time, elongation time [14], mean chromosome search time [15] etc. that can be tested experimentally. In this work, by extending the two state model proposed earlier by Hill [12], we study how the length dependent catastrophe rate affects the length distribution of microtubules. Motivated by their own observation, authors of [9] have proposed a length-dependent two-state model in which the catastrophe rate depends linearly on the microtubule length [16]. Following a continuum approach, they obtain microtubule length distributions and use these distributions further to obtain positional information regarding

the preferential cite for the future growth of the cell. In view of the relevance of the distributions, we are motivated to adopt a discrete formulation to obtain exact expressions of various length distribution functions. The length distribution obtained in [16] has a Gaussian form and our results agree with those of [16] under a special condition satisfied by the growth and catastrophe rates and the microtubule length.

The discrete description, unlike the continuum approach involving two partial differential equations, requires two infinite sets of coupled first order dynamical equations. Since further consideration of the internal protofilament structure of the microtubule would lead to more complexity, we have considered a microtubule to be a polymer of a single protofilament as a first approximation. Given the fact that the longitudinal bonds within a protofilament are strong in comparison with the lateral interaction [17], it is possible to extend the model by taking neighboring protofilaments into account. However, it may be worth noting that considering a "gating rescue" effect from the neighboring protofilament as done for the composite model of [11] leads to a behavior qualitatively similar to the single protofilament case. Other models of polymerization dynamics with length dependent attachment and detachment rates exist [18], but these models do not take into account the persistent nature of growth and shrinkage. In view of this, the present analysis, allows a direct comparison with the results of [12] in the steady-state.

The evolution equations are written for p_n^+ and p_n^- which are probability densities of having microtubules of length n in a growing or a shrinking phase respectively. The evolution equations for these probability densities are

$$\frac{dp_n^+}{dt} = r_a p_{n-1}^+ + r_{-+} p_n^- - (r_{+-} n + r_a) p_n^+, \quad n \geq 2, \quad (1)$$

$$\frac{dp_n^-}{dt} = r_d p_{n+1}^- + r_{+-} n p_n^+ - (r_d + r_{-+}) p_n^-, \quad n \geq 1. \quad (2)$$

Here, r_a , r_d , r_{+-} and r_{-+} denote the tubulin attachment rate, tubulin detachment rate, catastrophe rate and the rescue rate respectively. As seen in these equations, the catastrophe rate, $r_{+-} n$, for transition from p_n^+ to p_n^- is proportional to the microtubule length, n .

II. LENGTH INDEPENDENT CATASTROPHE RATE: CORRESPONDENCE WITH PREVIOUS RESULTS

Here we consider the case where the catastrophe rate is independent of the length of the microtubule and find correspondences with the results of reference [12]. The steady-state recurrence relations satisfied by the probability densities are

$$r_a p_{n-1}^+ + r_{-+} p_n^- - (r_{+-} + r_a) p_n^+ = 0 \quad \text{for } n \geq 2 \quad (3)$$

$$r_d p_{n+1}^- + r_{+-} p_n^+ - (r_d + r_{-+}) p_n^- = 0 \quad \text{for } n \geq 1. \quad (4)$$

Initially, we assume that p_1^+ remains constant at a given value. We use the generating function method to find the dependence of the probability densities on the microtubule length. The generating functions defined as

$$G(x) = \sum_{n=0}^{\infty} x^n p_{n+2}^+, \quad H(x) = \sum_{n=0}^{\infty} x^n p_{n+2}^- \quad (5)$$

satisfy the following equations

$$[r_a x - (r_{+-} + r_a)] G(x) + r_{-+} H(x) = -r_a p_1^+ \quad (6)$$

$$[r_d - (r_d + r_{-+}) x] H(x) + r_{+-} x G(x) = (r_d + r_{-+}) p_1^- - r_{+-} p_1^+. \quad (7)$$

Writing these equations in the matrix form as

$$\mathcal{A} \mathcal{G} = \mathcal{B}, \quad (8)$$

where

$$\mathcal{G} = \begin{pmatrix} G(x) \\ H(x) \end{pmatrix},$$

$$\mathcal{A} = \begin{pmatrix} r_a x - (r_{+-} + r_a) & r_{-+} \\ r_{+-} x & r_d - (r_d + r_{-+}) x \end{pmatrix}$$

and

$$\mathcal{B} = \begin{pmatrix} -r_a p_1^+ \\ (r_d + r_{-+}) p_1^- - r_{+-} p_1^+ \end{pmatrix},$$

we find the solutions for $G(x)$ and $H(x)$ as

$$G(x) = \frac{1}{|\mathcal{A}|} [-\{r_d - (r_d + r_{-+}) x\} r_a p_1^+ + r_{-+} r_{-+} p_1^+ - r_{-+} (r_d + r_{-+}) p_1^-], \quad (9)$$

$$H(x) = \frac{1}{|\mathcal{A}|} [r_{+-} r_a p_1^+ x + \{r_a x - (r_a + r_{+-})\} \times \{(r_d + r_{-+}) p_1^- - r_{+-} p_1^+\}], \quad (10)$$

where $|\mathcal{A}| = (1-x)[r_a(r_d + r_{-+})x - r_d(r_a + r_{+-})]$ is the determinant of matrix \mathcal{A} . Clearly, matrix \mathcal{A} is singular at $x = 1$ and this poses a question on the basic assumption of the steady-state. However, this singularity is a removable one if one considers the time evolution of the probability density, p_1^+ , and the probability density of nucleating sites p_0 . With the following evolution equations [12],

$$\frac{dp_1^+}{dt} = r_a p_0 + r_{-+} p_1^- - (r_a + r_{+-}) p_1^+ \quad (11)$$

$$\frac{dp_0}{dt} = -r_a p_0 + r_d p_1^-, \quad (12)$$

one obtains the steady-state conditions $p_1^- = \frac{r_a}{r_d} p_0$ and $p_1^+ = D_0 p_0$, with $D_0 = \frac{r_a(r_{-+} + r_d)}{r_d(r_{-+} + r_a)}$. It is straightforward

to see that the singularities in (9) and (10) disappear once the ratio $p_1^+/p_1^- = \frac{r_{-+}+r_d}{r_{+-}+r_a}$ is substituted in (8). Subsequent algebra leads to the steady-state probability densities

$$p_n^+ = D_0^n p_0, \quad \text{and} \quad p_n^- = \frac{r_a}{r_d} D_0^{n-1} p_0 \quad (13)$$

as given in [12]. It is important to note that the ratio p_n^+/p_n^- as obtained here does not match with the results of Appendix A of [16]. (Also see the discussion below.) The steady-state probability density p_n^+ decays exponentially with n as

$$p_n^+ = p_0 \exp[-\alpha n], \quad \text{with} \quad \alpha = -\ln D_0, \quad (14)$$

if α is positive. In general, with constant p_1^+ , the singularity at $x = 1$ is removable provided p_1^- evolves with time such that the above ratio of p_1^+/p_1^- is satisfied. This ratio is approached as $t \rightarrow \infty$ with a correction disappearing exponentially with time.

III. LENGTH DEPENDENT CATASTROPHE RATE

In order to analyze the evolution equations with length dependent catastrophe rate, we consider the generating functions as given in (5) with time dependent probability densities. The generating functions are, in this case, time dependent. Summing (1) and (2) over n , we obtain the following differential equations for $G(x, t)$ and $H(x, t)$.

$$\begin{aligned} \frac{dp_1^-(t)}{dt} + x \frac{dH(x, t)}{dt} &= [r_d - (r_d + r_{-+})x]H(x, t) + \\ &2r_{+-}xG(x, t) + r_{+-}x^2G'(x, t) + \\ &(r_{+-}p_1^+ - (r_d + r_{-+})p_1^-), \quad \text{and} \end{aligned} \quad (15)$$

$$\begin{aligned} \frac{dG(x, t)}{dt} &= r_a p_1^+ + (-r_a - 2r_{+-} + r_a x)G(x, t) - \\ &r_{+-}xG'(x, t) + r_{-+}H(x, t). \end{aligned} \quad (16)$$

Here, prime denotes derivative with respect to x . One could also directly consider the steady-state equations and obtain the probability densities by a transfer matrix approach. However, since its use is difficult in the length-dependent case, we follow the generating function method here. Using Eq. (2) for $n = 1$, all the x independent terms of equation (15) can be together expressed in terms of $p_2^-(t)$. Taking Laplace transform of Eqs. (15) and (16), we have

$$\begin{aligned} \tilde{H}(x, s)[sx - r_d(1 - h_1x)] &= -r_d \tilde{p}_2^-(s) + \\ &2r_{+-}x\tilde{G}(x, s) + r_{+-}x^2\tilde{G}'(x, s), \quad \text{and} \end{aligned} \quad (17)$$

$$\begin{aligned} \tilde{G}(x, s)[s + r_a(1 - x) + 2r_{+-}] &+ r_{+-}x\tilde{G}'(x, s) - \\ r_{-+}\tilde{H}(x, s) &= r_a \tilde{p}_1^+(s), \end{aligned} \quad (18)$$

where $h_1 = \frac{r_d+r_{-+}}{r_d}$ and $\tilde{f}(x, s) = \int_0^\infty dt e^{-st} f(x, t)$. While obtaining these equations, we have assumed $G(x, t = 0) = H(x, t = 0) = 0$ i.e. initially there are no growing or shrinking polymers of length $n \geq 2$. These two equations can be combined to obtain a single differential equation for $\tilde{G}(x, s)$ as

$$\begin{aligned} \tilde{G}'(x, s)[(r_{+-}s + r_d r_{+-})x^2 - r_d r_{+-}x] &+ r_d r_{-+} \tilde{p}_2^-(s) + \\ \tilde{G}(x, s)[A + Bx + Cx^2] &= r_a [sx - r_d(1 - h_1x)] \tilde{p}_1^+(s), \end{aligned} \quad (19)$$

where

$$A = -sr_d - r_a r_d - 2r_{+-}r_d, \quad (20)$$

$$B = s^2 + sr_d + sr_{-+} + r_a s + r_a r_d + r_a r_d h_1 + \\ 2r_{+-}s + 2r_{+-}r_d, \quad \text{and} \quad (21)$$

$$C = -r_a s - r_a r_d h_1. \quad (22)$$

In order to obtain the steady state behavior, we use the final value theorem which is based on the assumption that the steady-state generating function $G(x) = G(x, t \rightarrow \infty)$ exists and is given by $G(x, t \rightarrow \infty) = \lim_{s \rightarrow 0} s \tilde{G}(x, s)$. The same is assumed to be valid for other functions $\tilde{p}_1^+(s)$ and $\tilde{p}_2^-(s)$. As $s \rightarrow 0$, Eq. (19) becomes singular at $x = 1$. However, as in the length independent case, this singularity is a removable one when the appropriate steady-state expressions for p_1^+ and p_1^- are used. After these substitutions, the steady-state generating function satisfies the following equation

$$(r_{+-}r_d)x \frac{dG}{dx} + (d_1 - d_2x)G(x) = d_3, \quad \text{where} \quad (23)$$

$$\begin{aligned} d_1 &= r_d(r_a + 2r_{+-}), \quad d_2 = r_a(r_d + r_{-+}) \quad \text{and} \\ d_3 &= p_1^+ r_a(r_d + r_{-+}). \end{aligned} \quad (24)$$

This inhomogeneous equation has a solution of the form $G(x) = G_c(x) + G_p(x)$ having a complementary part

$$G_c(x) = C_0 x^{-\frac{d_1}{r_{+-}r_d}} \exp\left[\frac{d_2}{r_{+-}r_d}x\right] \quad (25)$$

with C_0 as a constant and a particular integral for which a series of the form in Eq. (5) can be considered. Eq. (24) has a singularity at $x = 0$ and this results in a singularity of the complementary solution at $x = 0$. Since a catastrophe rate proportional to the microtubule length is expected to decrease the probability densities than those of the length independent case and a diverging solution for the generating function is unlikely, we choose $C_0 = 0$. The particular solution gives the probability densities as

$$p_2^+ = d_3/d_1, \quad (26)$$

$$p_n^+ = \frac{d_3}{d_1} \frac{d_2^{n-2}}{\prod_{m=1}^{n-2} (d_1 + m r_{+-} r_d)} \quad \text{for } n > 2, \quad (27)$$

$$p_{n+2}^- = \frac{r_a}{r_d} p_{n+1}^+ \quad \text{for } n \geq 0. \quad (28)$$

Eq. (27), can be rewritten in the form

$$p_n^+ = \frac{d_3}{d_1} \left(\frac{d_2}{(r_{+-}r_d)} \right)^{n-2} \frac{\Gamma(d_1/(r_{+-}r_d) + 1)}{\Gamma((n-1) + d_1/(r_{+-}r_d))}, \quad (29)$$

where $\Gamma(x)$ is the usual Γ function of argument x . Hence, for large n , the exponential decay of (14) is modified as

$$p_n^+ \sim \exp[-\alpha' n - n \ln n], \quad (30)$$

with $\alpha' = \ln \frac{(r_{+-}r_d)}{d_2} - 1$. As Figs. 1 and 2 show, the decay of p_n^+ of p_n^- , dominated by an $\exp[-n \ln n]$ type term, is much faster than that of the length independent dynamics [19]. The ratio p_n^-/p_{n-1}^+ , however, remains same as that of the length independent case. In Figs. 3 and 4, we have plotted the probability densities for different attachment rates. Fig. 4 shows an overall increase of p_n^- with the attachment rate. This seems to be a consequence of rapid polymerization and hence an enhanced transition of microtubules from growing to the shrinking phase. With the present form of distributions of growing and shrinking microtubules, the average length of microtubules is given by $n \approx 26.4$ for $r_a = 14.37 \text{ sec}^{-1}$ and other parameter values same as provided in Fig. 3.

In a continuum description of the microtubule length, one may have the following steady-state differential equations [16]

$$-r_a a \frac{\partial p^+(L)}{\partial L} + r_{+-} p^-(L) - r_{+-} \frac{L}{a} p^+(L) = 0 \quad (31)$$

$$r_d a \frac{\partial p^-(L)}{\partial L} + r_{+-} \frac{L}{a} p^+(L) - r_{+-} p^-(L) = 0, \quad (32)$$

where a is the length of the tubulin dimer. In case of bounded solutions for $p^+(L)$ and $p^-(L)$, it is found that $\frac{p^-(L)}{p^+(L)} = \frac{r_a}{r_d}$ [16]. Eq. (28) and also the corresponding eq. in the length independent case (Eq. (13)) are different from this. Although (28) and its continuum analogue mentioned above are simple balance equations in terms of the rate parameters, the subtle difference between them becomes important here unlike the length independent case. In order to find the reason for such difference, we do a Taylor expansion of Eq. (28) in the dimer length, a . Retaining terms up to first order in a , the ratio appears as $\frac{p^-(L)}{p^+(L)} = \frac{r_a}{r_d} (1 - a \frac{1}{p^+(L)} \frac{\partial p^+(L)}{\partial L})$. Replacing the first order term using Eq. (31), it can be seen that the ratio becomes same as that of [16] provided $r_{+-}/r_a \ll a/L = 1/n$. Rather than referring this as a condition for validity of the continuum approximation, it is more appropriate to mention that this condition expresses a competition between the catastrophe and the growth rate which, as we shall see below, distinguish two regimes with two different kinds of probability distributions.

That the distribution in (27) finally becomes a Gaussian distribution for $r_{+-}/r_a \ll a/L$, can be seen by approximating the logarithm of the product in the denominator of (27) in the following way.

$$\ln \prod_{m=1}^{n-2} (d_1 + m r_{+-} r_d) =$$

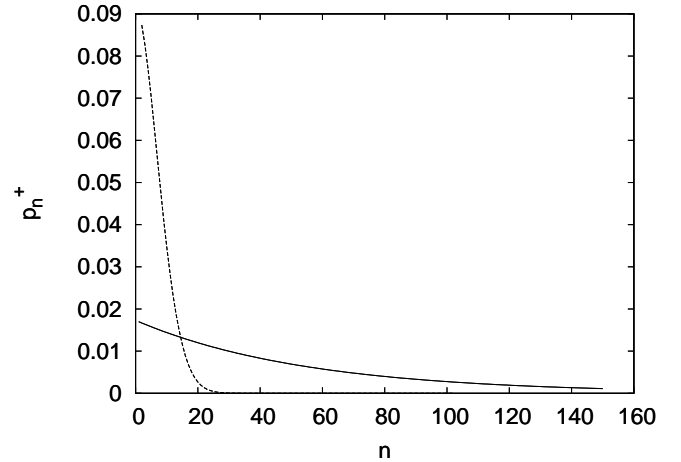


FIG. 1: Steady-state probability densities for growing microtubules are plotted with length. Solid and dashed lines correspond to length independent and length dependent catastrophe rates respectively. Parameter values used for the plot are $r_a = 10 \text{ s}^{-1}$, $r_d = 40 \text{ s}^{-1}$, $r_{+-} = 0.02 \text{ s}^{-1}$ and $r_{+-} = 0.19 \text{ s}^{-1}$.

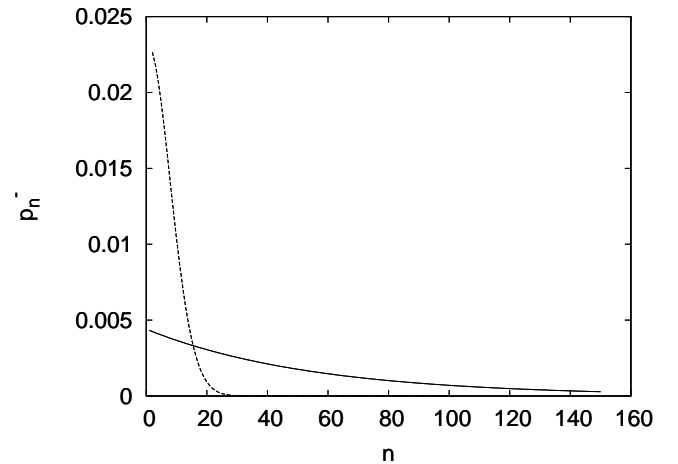


FIG. 2: Steady-state probability densities for shrinking microtubules are plotted with length. Solid and dashed lines have the same meaning as in Fig 1. Parameter values are same as those of Fig. 1.

$$\begin{aligned} (n-2) \ln d_1 + \sum_{m=1}^{n-2} \ln \left(1 + m \frac{r_{+-} r_d}{d_1} \right) &\approx \\ (n-2) \ln d_1 + \int_0^L dx \ln \left(1 + \frac{x r_{+-} r_d}{a d_1} \right) &\approx \\ (n-2) \ln d_1 + \frac{r_{+-}}{(r_a + 2r_{+-})a} \int_0^L dx x. &\quad (33) \end{aligned}$$

Since $r_{+-}/r_a \ll a/L$, we have used $\ln(1+x) \approx x$ to approximate the integrand. It is straightforward now to see that (33) finally leads to a Gaussian distribution for the length. $\exp[-n \ln n]$ form of Eq. (30), on

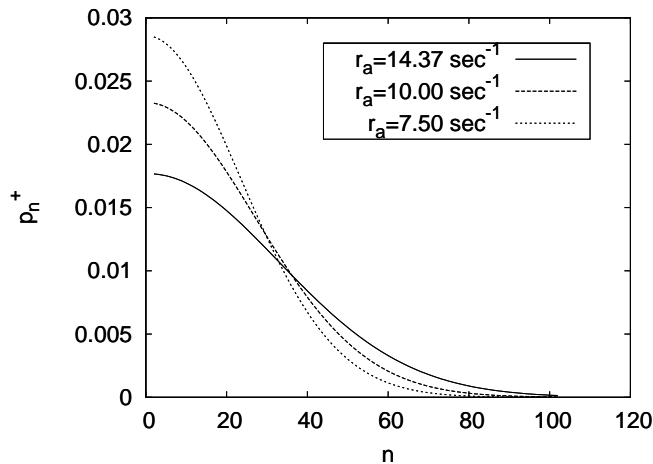


FIG. 3: Steady-state probability densities for growing microtubules are plotted as a function of length for different attachment rates. Values of parameters other than r_a are $r_d = 37.5 \text{ s}^{-1}$, $r_{+-} = 0.014 \text{ s}^{-1}$ and $r_{-+} = 0.044 \text{ s}^{-1}$.

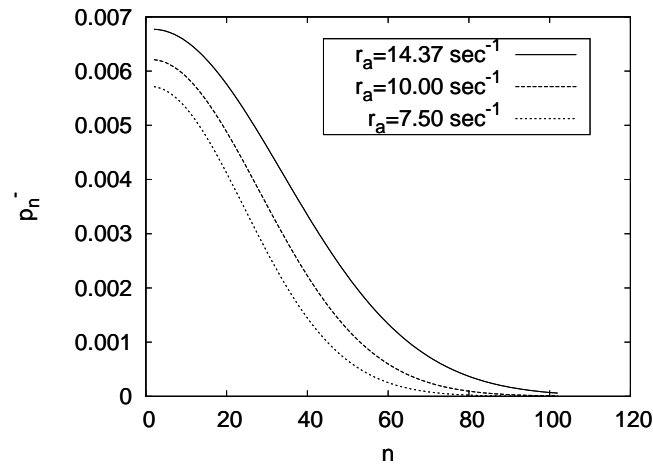


FIG. 4: Steady-state probability densities for shrinking microtubules are plotted with length for different attachment rates. Parameter values are same as those of Fig. 3.

the other hand, follows in the opposite situation where $1/n = a/L \ll r_{+-}/r_a$. This analysis shows that the higher is the growth rate the quicker is the fall of the probability distribution of growing polymers. This seems to be a consequence of the fact that a rapid growth induces more frequent catastrophe.

IV. SUMMARY

It has been found that the catastrophe frequency becomes dependent on the microtubule length due to the activity of depolymerases belonging kinesin-8 family. Here, we consider a two-state model of growing and shrinking microtubules having a catastrophe rate that increases linearly with the length of the microtubule. Following a discrete approach, we study how the steady state probability densities p_n^+ and p_n^- of growing and shrinking polymers, respectively, of length n , vary with length. Our results show that, for large n , the decay of the probability densities with n is dominated by an $\exp[-n \ln n]$ type of term as compared to an $\exp[-\alpha n]$ kind of decay in the length independent catastrophe case.

Acknowledgement Financial support from the Department of Science and Technology, India is gratefully acknowledged.

-
- [1] Lodish *et al.* Molecular Cell Biology, 5th ed., W. H. Freeman and Company, NY, 2004.
 - [2] T. Mitchison and M. Kirschner, Nature **312**, 232 (1984); T. Mitchison and M. Kirschner, Nature **317**, 237 (1984).
 - [3] M. -F. Carlier and D. Pantaloni, Biochemistry **20**, 1918 (1981).
 - [4] H. Flyvbjerg, T. E. Holy and S. E. Leibler, Phys. Rev. Lett. **73**, 2372 (1994); T. Antal, P. L. Krapivsky and S. Redner, J. Stat. Mech. **5** L05004 (2007).
 - [5] J. Howard and A. A. Hyman, Curr. Opin. in Cell Biol. **19**, 31 (2007).
 - [6] M. Dogterom *et al.*, J. Cell. Biol. **133**, 125 (1996).
 - [7] V. Varga *et al.* Nat. Cell. Biol. **8**, 957 (2006); V. Varga *et al.* Cell **138**, 1174 (2009).
 - [8] M. K. Gardner *et al.*, Cell **135**, 894 (2008).
 - [9] C. Tischer, D. Brunner and M. Dogterom, Mol. Syst. Biol. **5**, 250 (2009).
 - [10] B. L. Sprague *et al.*, Biophys. J **84**, 3529 (2003); R. Wollman *et al.*, Curr. Biol. **15**, 828 (2005).
 - [11] L. Brun *et al.*, Proc. Natl. Acad. Sci. USA **106**, 21173 (2009).
 - [12] T. L. Hill, Proc. Natl. Acad. Sci **81**, 6728 (1984); R. J. Rubin, *ibid* **85**, 446 (1988).
 - [13] M. Dogterom and S. Leibler, Phys. Rev. Lett. **70**, 1347 (1993).
 - [14] D. J. Bicout, Phys. Rev. E **56**, 6656 (1997); D. J. Bicout and R. J. Rubin, Phys. Rev. E **59**, 913 (1999).
 - [15] M. Gopalakrishnan and B. S. Govindan, e-print arxiv:

- 0904.0111.
- [16] C. Tischer, P. R. Wolde and M. Dogterom, *Biophys. J.* **99**, 726 (2010).
- [17] V. Van Buren, D. J. Odde and L. Cassimeris, *Proc. Natl. Acad. Sci. USA* **99**, 6035 (2002)
- [18] I. Mazilu, G. Zamora and J. Gonzalez, *Physica A* **389**, 419 (2010).
- [19] Values of the parameters, used for the figures, are obtained from references of experimental works provided in [16].